https://doi.org/10.5194/hess-2021-29
Preprint. Discussion started: 11 March 2021

Hydrology and Earth System Sciences
Open Access
Discussions

Effects of aquifer geometry on seawater intrusion in annulus segment island aquifers

Zhaoyang Luo[1,2], Jun Kong[1,3,#], Chengji Shen[1], Pei Xin[1], Chunhui Lu[1], Ling Li[4], David Andrew Barry[2]

[1]State Key Laboratory of Hydrology-Water Resources and Hydraulic Engineering, Hohai University, Nanjing, China

[2]Ecological Engineering Laboratory (ECOL), Environmental Engineering Institute (IIE), Faculty of Architecture, Civil and Environmental Engineering (ENAC), École Polytechnique Fédérale de Lausanne (EPFL), Lausanne, Switzerland

[3]Jiangsu Key Laboratory of Coast Ocean Resources Development and Environment Security, Hohai University, Nanjing, China

[4]School of Engineering, Westlake University, Hangzhou, China

[#]Corresponding author: Jun Kong (kongjun999@126.com)

https://doi.org/10.5194/hess-2021-29
Preprint. Discussion started: 11 March 2021

Hydrology and Earth System Sciences Discussions

Abstract

Seawater intrusion in island aquifers is considered analytically, specifically for annulus segment aquifers (ASAs), i.e., aquifers that (in plan) have the shape of an annulus segment. Based on the Ghijben-Herzberg and hillslope-storage Boussinesq equations, analytical solutions are derived for steady-state seawater intrusion for ASAs, with a focus on the freshwater-seawater interface and its corresponding watertable elevation. These analytical solutions, after comparing their predictions with experimental data, are employed to investigate the effects of aquifer geometry on seawater intrusion in island aquifers. Three different geometries of ASA are compared: convergent (smaller side facing the lagoon), rectangular and divergent (larger side facing the sea). The results show that the predictions from the analytical solutions are in well agreement with the experimental data for both recharge events. In addition, seawater intrusion is most extensive in divergent aquifers, and conversely for convergent aquifers. Accordingly, the watertable elevation is lowest in divergent aquifers and highest in convergent aquifers. Moreover, the effects of aquifer geometry on the freshwater-seawater interface and watertable elevation vary with aquifer width and distance to the no-flow boundary. Both a larger aquifer width and distance to the no-flow boundary weaken the effects of aquifer geometry and hence lead to a smaller deviation of seawater intrusion between the three geometries.

Keywords: sharp-interface; steady-state; convergent aquifer; divergent aquifer; rectangular aquifer

https://doi.org/10.5194/hess-2021-29
Preprint. Discussion started: 11 March 2021

Hydrology and Earth System Sciences
Open Access
Discussions

Key Points

- Analytical solutions of steady-state seawater intrusion are derived for annulus segment aquifers
- Among three different aquifer geometries, divergent aquifers have lowest watertable and hence most extensive seawater intrusion
- Aquifer geometry effects on seawater intrusion depend on the aquifer width and distance from the circle center to the no-flow boundary

https://doi.org/10.5194/hess-2021-29
Preprint. Discussion started: 11 March 2021

Hydrology and Earth System Sciences Discussions

1. Introduction

Islands are extensively distributed in global oceans and are considered as vulnerable places due to sea-level rise and human population growth. According to a recent estimate, there are approximately 65 million people living in oceanic islands, where fresh groundwater may be the only source of freshwater (Thomas et al., 2020). Fresh groundwater stored on oceanic islands is mainly recharged from precipitation and its availability can be impacted by a variety of factors, including island topography, rainfall patterns, tides, episodic storms and human activities (White & Falkland, 2010; Storlazzi et al., 2018). Among these, seawater intrusion is another important issue that greatly affects oceanic island freshwater storage and is thus of considerable interest (e.g., Werner et al., 2017; Lu et al., 2019; Memari et al., 2020).

Different from coastal aquifers where seawater intrudes into freshwater from one direction only, seawater intrusion occurs from two directions for narrow strip islands and from all directions for circular islands. Over the past few decades, seawater intrusion in oceanic islands has been extensively investigated in multiple ways, either directly by field observations (e.g., Röper et al., 2013; Post et al., 2019), or indirectly by experimental measurements (e.g., Stoeckl et al., 2015; Bedekar et al., 2019; Memari et al., 2020), numerical simulations (e.g., Lam, 1974; Gingerich et al., 2017; Liu & Tokunaga, 2019), and analytical solutions (e.g., Fetter, 1972; Ketabchi et al., 2014; Lu et al., 2019). Among these, analytical solutions are effective tools to assess the extent of seawater intrusion, despite that they cannot incorporate complex factors (e.g., dispersive mixing and transient oceanic dynamics) (Werner et al., 2013). The advantages of analytical solutions are that (1) they are rapidly and easily computed, and (2) they give

https://doi.org/10.5194/hess-2021-29
Preprint. Discussion started: 11 March 2021

Hydrology and Earth System Sciences
Open Access
Discussions
EGU

explicit relationships between parameters that influence seawater intrusion.

Based on the Dupuit-Forchheimer approximation (i.e., ignoring vertical flow) and the Ghijben-Herzberg equation (Drabbe & Badon Ghijben, 1889, English translation given by Post (2018); Herzberg, 1901), Fetter (1972) presented analytical solutions describing the freshwater-seawater interface location and watertable elevation in a circular island. Bailey et al (2010) further compared these single-layer analytical solutions with field measurements, indicating that the analytical solutions perform well in estimating the freshwater-seawater interface location and watertable elevation. Fetter's (1972) solutions formed the fundament for many analytical studies aimed at seawater intrusion in island aquifers. Based on this single-layer analytical theory, Chesnaux and Allen (2008) and Greskowiak et al. (2013) developed analytical solutions to predict the steady-state groundwater age distribution in freshwater lenses. In addition, using the single-layer analytical solutions, Morgan and Werner (2014) proposed vulnerability indicators of freshwater lenses under sea-level rise and recharge change.

Since aquifers are usually heterogeneous in reality, the single-layer analytical solutions are extended to two-layer island aquifers subsequently. Vacher (1988) derived solutions for the freshwater-seawater interface location and watertable elevation for infinite-strip islands composed of different layers. Dose et al. (2014) carried out laboratory experiments to validate analytical solutions proposed by Fetter (1972) and Vacher (1988) and confirmed their reliability. Ketabchi et al. (2014) extended Fetter (1972)'s analytical solutions to calculate the freshwater-seawater interface location and watertable elevation in two-layer circular islands subject to sea-level rise. Their results indicated that land-surface inundation caused by sea-level rise has a

https://doi.org/10.5194/hess-2021-29
Preprint. Discussion started: 11 March 2021

considerable impact on the fresh groundwater lens. The analytical solutions of Ketabchi et al. (2014) and Vacher (1998) assumed an island with two horizontal layers. More recently, Lu et al. (2019) derived analytical solutions for the freshwater-seawater interface location and watertable elevation for both strip and circular islands with two adjacent layers, i.e., a less permeable slice along the shoreline of an island, and a more permeable zone inland. For more studies associated with seawater intrusion in oceanic islands, readers are referred to the comprehensive review of Werner et al. (2017).

All the abovementioned analytical solutions apply to either strip or circular islands. According to the classification of sand dune developed by Stuyfzand (1993; 2017), there are different layouts, e.g., Figure 1, where the shape of the island is an annulus segment, instead of a strip or circle. This configuration is widely distributed in atolls (i.e., circular chains of islands surrounding a central lagoon) as found in the Pacific and Indian Oceans (Werner et al., 2017; Duvat, 2019). Nevertheless, no analytical solutions of seawater intrusion have been developed for annulus segment aquifers (ASAs). In general, ASAs are conceptually treated as a 2D cross section like strip islands (e.g., Ayers & Vacher, 1986; Underwood et al., 1992; Bailey et al., 2009; Werner et al., 2017). Evidently, topography plays an important role in groundwater flow and hence seawater intrusion (e.g., Zhang et al., 2016; Liu & Tokunaga, 2019). It remains unclear whether the analytical solutions of seawater intrusion for strip islands are appropriate for ASAs and how island geometry affects the freshwater-seawater interface location and watertable elevation of ASAs.

In this study, we derive analytical solutions of the steady-state seawater intrusion for ASAs, with a focus on the freshwater-seawater interface location and its corresponding watertable elevation. After comparing their predictions with experimental data compiled from Memari et al. (2020), the analytical solutions are employed to investigate the effects of aquifer geometry on the freshwater-seawater interface location and watertable elevation in ASAs.

2. Conceptual Model

Figure 2 shows the conceptual model of an ASA (a slice of atoll islands). The plan view of the model domain is represented as a sector (*EFGH*) with an angle θ (Figure 2a). Radial flow only is considered. The sea (*EF*) and lagoon (*HG*) boundaries are located at $L+L_0$ [L] and L_0 [L] from the circle center, respectively. Since the longitudinal length is much longer than the lateral length for an atoll island in reality (Werner et al., 2017), it can be expected that seawater intrusion from lateral side would have negligible influence on that from longitudinal side, especially for the middle part of an ASA. In order to facilitate analytical derivations, therefore, *EH* and *FG* are treated as no-flow boundaries. It should be noted that assuming lateral boundary as a no-flow boundary (e.g., *EH* and *FG*) has been widely adopted in previous studies related to freshwater lenses on atoll islands (e.g., Ayers & Vacher, 1986; Underwood et al., 1992; Bailey et al., 2009; Werner et al., 2017). The side view of the model domain is conceptualized as a rectangle (*ABCD*) along the radial direction with dimensions of L [L] (width) × d [L] (height) (Figure 2b,c). *AD* and *BC* are impermeable base and land surface boundary, respectively.

To facilitate analytical derivations, both the sea and lagoon water levels are H_s [L], which results in a no-flow boundary (water divide) between the sea and lagoon. For simplicity, the segment between the sea and no-flow boundaries is referred to as Unit 1, whereas the

https://doi.org/10.5194/hess-2021-29
Preprint. Discussion started: 11 March 2021

segment between the no-flow and lagoon boundaries is referred to as Unit 2. The widths of Units 1 and 2 are l_1 [L] and l_2 [L], respectively. In addition, the flow is asymmetrical in Units 1 and 2, with divergent flow (the aquifer length *w* [L] increases along the flow direction) in Unit 1 and convergent flow (the aquifer length *w* [L] decreases along the flow direction) in Unit 2.

The *x*-*z* coordinate origin is placed at the intersection of the no-flow boundary and impermeable base, with the *x*-axis horizontally pointing to the circle center and *z*-axis vertically upward. ϕ [L] is the watertable height. h [L] is the vertical distance between the watertable and the interface. h_s [L] is the vertical distance between the sea level and the interface, and $h_c = H_s - h_s$ [L] is the vertical distance from the impermeable base to the interface. Recharge into the saturated zone is assumed to be uniform with value of N [LT^{-1}]. There are two possibilities for the interface tip location: above the aquifer bed (Figure 2b) and on the aquifer bed (Figure 2c). For the condition with the interface tip on the aquifer bed, the interface tip locations in Units 1 and 2 are denoted as x_{t1} [L] and x_{t2} [L], respectively. Consistent with previous studies (e.g., Ketabchi et al., 2014; Lu et al., 2016; 2019), the following assumptions are made: (1) the flow system is steady state, (2) a sharp interface exists between freshwater and seawater, (3) aquifer hydraulic properties are homogeneous and isotropic, (4) unsaturated flow is neglected, (5) recharge is smaller than the saturated hydraulic conductivity (no ponding), and (6) vertical flow is neglected in the saturated zone (i.e., Dupuit-Forchheimer approximation).

https://doi.org/10.5194/hess-2021-29
Preprint. Discussion started: 11 March 2021

3. Analytical Solutions Derivation

Groundwater flow in an ASA (Figure 2) can be described as (Paniconi et al., 2003; Troch et al., 2003),

$$-\frac{\partial}{\partial x}(wq)+Nw=\frac{\partial S}{\partial t} \tag{1}$$

where q [L^2T^{-1}] is the Darcy flux per unit length along the aquifer; S [L^2] is the total water storage per unit distance along the aquifer, and t [T] is time. Equation (1) is derived from the hillslope-storage Boussinesq equation reformulated in terms of soil water storage rather than watertable elevation, as widely used previously (e.g., Stagnitti et al., 1986; Troch et al., 2003; Hilberts et al., 2005; Kong et al., 2016; Luo et al., 2018). At steady state, equation (1) reduces to,

$$-\frac{\partial}{\partial x}(wq)+Nw=0 \tag{2}$$

According to Darcy's law and the Dupuit-Forchheimer approximation, the freshwater flux in the aquifer segment between the seaward boundary and interface tip can be calculated as,

$$q=-\int_{h_c}^{\phi}K_s\frac{d\phi}{dx}dz \tag{3}$$

where K_s [LT^{-1}] is the saturated hydraulic conductivity.

3.1. Interface Tip above the Aquifer Bed

We first consider the situation where the interface tip is above the aquifer bed (Figure 2b). In Unit 1 where $w=\theta(L_0+l_2-x)$, substituting equation (3) into equation (2) and then integrating gives,

$$-\frac{1}{2}\left[(L_0+l_2-x)^2-(L_0+l_2)^2\right]N=-(L_0+l_2-x)\int_{h_c}^{\phi}K_s\frac{d\phi}{dx}dz \tag{4}$$

According to the Ghijben-Herzberg equation, the vertical thickness of the freshwater zone

(h) in the interface zone is given by,

$$h = (1+\alpha)(\phi - H_s) \tag{5}$$

where $\alpha = \rho_f / (\rho_s - \rho_f)$ [-] is the dimensionless density difference, with ρ_f [ML^{-3}] and ρ_s [ML^{-3}] being the densities of freshwater and seawater, respectively.

Substitution of equation (5) into equation (4) yields,

$$-\frac{1}{2}\left[(L_0 + l_2 - x)^2 - (L_0 + l_2)^2\right]N = -K_s(L_0 + l_2 - x)(1+\alpha)(\phi - H_s)\frac{d\phi}{dx} \tag{6}$$

Rearranging equation (6) produces,

$$-\frac{(L_0 + l_2 - x)N}{2} + \frac{N(L_0 + l_2)^2}{2(L_0 + l_2 - x)} = -K_s(1+\alpha)(\phi - H_s)\frac{d\phi}{dx} \tag{7}$$

Integrating equation (7) leads to,

$$-\frac{(L_0 + l_2)^2 N}{2}\ln(L_0 + l_2 - x) - \frac{1}{2}(L_0 + l_2)Nx + \frac{1}{4}Nx^2 + C_1 = -K_s(1+\alpha)\frac{(\phi - H_s)^2}{2} \tag{8}$$

where C_1 is the integration constant and can be determined by the sea boundary condition (i.e., $x = -l_1$, $\phi = H_s$),

$$C_1 = \frac{(L_0 + l_2)^2 N}{2}\ln(L_0 + l_2 + l_1) - \frac{1}{2}(L_0 + l_2)l_1 N - \frac{1}{4}l_1^2 N \tag{9}$$

The relation between h_s and ϕ is given by,

$$h_s = \alpha(\phi - H_s) \tag{10}$$

Combining equation (8) with equation (10) and eliminating ϕ yield,

$$-\frac{(L_0 + l_2)^2 N}{2}\ln(L_0 + l_2 - x) - \frac{1}{2}(L_0 + l_2)Nx + \frac{1}{4}Nx^2 + C_1 = -K_s(1+\alpha)\frac{h_s^2}{2\alpha^2} \tag{11}$$

Equation (11) can be adopted to calculate the freshwater-seawater interface location in Unit 1 if both l_1 and l_2 are determined.

https://doi.org/10.5194/hess-2021-29
Preprint. Discussion started: 11 March 2021

Equation (8) can also apply to Unit 2 by replacing C_1 with C_2,

$$-\frac{(L_0+l_2)^2 N}{2}\ln(L_0+l_2-x)-\frac{1}{2}(L_0+l_2)Nx+\frac{1}{4}Nx^2+C_2=-K_s(1+\alpha)\frac{(\phi-H_s)^2}{2} \quad (12)$$

where C_2 is chosen to satisfy the lagoon boundary condition ($x=l_2$, $\phi=H_s$),

$$C_2=\frac{(L_0+l_2)^2 N}{2}\ln(L_0)+\frac{1}{2}(L_0+l_2)l_2 N-\frac{1}{4}l_2^2 N \quad (13)$$

Combining equation (10) and equation (12) and eliminating ϕ yield,

$$-\frac{(L_0+l_2)^2 N}{2}\ln(L_0+l_2-x)-\frac{1}{2}(L_0+l_2)Nx+\frac{1}{4}Nx^2+C_2=-K_s(1+\alpha)\frac{h_s^2}{2\alpha^2} \quad (14)$$

Similarly, equation (14) can be adopted to calculate the freshwater-seawater interface location in Unit 2 if l_2 is determined. As mentioned before, since the sea level and lagoon water level are assumed to be the same, a no-flow boundary exists between the sea and lagoon, i.e.,

$$x=0,\ (h_s)_{unit1}=(h_s)_{unit2} \quad (15)$$

Combining equation (11) and equation (14) with equation (15) leads to expressions for l_1 and l_2, respectively,

$$l_1=L+L_0-\sqrt{\frac{2LL_0+L^2}{2\ln(L+L_0)-2\ln(L_0)}} \quad (16)$$

$$l_2=\sqrt{\frac{2LL_0+L^2}{2\ln(L+L_0)-2\ln(L_0)}}-L_0 \quad (17)$$

As indicated by equations (16) and (17), the no-flow boundary between the sea and lagoon only depends on L and L_0 under steady state. For known l_1 and l_2, equations (11) and (14) can be employed to predict the freshwater-seawater interface location in Units 1 and 2, respectively. Once the interface location is determined, we can further calculate h and ϕ as

https://doi.org/10.5194/hess-2021-29
Preprint. Discussion started: 11 March 2021

follows,

$$h = \frac{1+\alpha}{\alpha} h_s \tag{18}$$

$$\phi = \frac{h_s}{\alpha} + H_s \tag{19}$$

3.2. Interface Tip on the Aquifer Bed

When the interface tip is on the aquifer bed, the location of the no-flow boundary remains the same as for the interface tip above the aquifer bed. The freshwater-seawater interface for Units 1 and 2 can be respectively determined by equations (11) and (14). Then we can calculate h at the aquifer segment between the sea boundary and the interface tip according to equation (18).

In order to calculate h for the aquifer segment between the interface tip and the no-flow boundary, the interface tip location should be determined first. At the interface tip ($x = x_{t1}$) of Unit 1, we have,

$$h_s = H_s \tag{20}$$

$$\phi = \frac{1+\alpha}{\alpha} H_s \tag{21}$$

By substituting equation (21) into equation (11), the interface tip location of Unit 1 can be obtained as,

$$-\frac{(L_0+l_2)^2 N}{2}\ln(L_0+l_2-x_{t1}) - \frac{1}{2}(L_0+l_2)Nx_{t1} + \frac{1}{4}Nx_{t1}^2 = -C_1 - K_s(1+\alpha)\frac{H_s^2}{2\alpha^2} \tag{22}$$

Let,

$$a = \frac{1}{4}N \tag{23a}$$

$$b = -\frac{1}{2}(L_0+l_2)N \tag{23b}$$

https://doi.org/10.5194/hess-2021-29
Preprint. Discussion started: 11 March 2021

$$c = -\frac{(L_0 + l_2)^2 N}{2} \tag{23c}$$

$$m = -C_1 - K_s(1+\alpha)\frac{H_s^2}{2\alpha^2} \tag{23d}$$

then equation (22) becomes,

$$ax_{t1}^2 + bx_{t1} + c\ln(L_0 + l_2 - x_{t1}) = m \tag{24}$$

Equation (24) can be easily solved by a root-finding method.

The freshwater discharge for the aquifer segment between the interface tip and the no-flow boundary can be calculated as,

$$-\frac{1}{2}\left[(L_0 + l_2 - x)^2 - (L_0 + l_2)^2\right]N = -(L_0 + l_2 - x)\int_0^{\phi} K_s \frac{d\phi}{dx} dz \tag{25}$$

Repeating the steps from equations (4) to (8) gives,

$$-\frac{(L_0 + l_2)^2 N}{2}\ln(L_0 + l_2 - x) - \frac{1}{2}(L_0 + l_2)Nx + \frac{1}{4}Nx^2 + C_3 = -\frac{K_s}{2}\phi^2 \tag{26}$$

where C_3 can be determined by substituting equation (21) to equation (26). Subsequently, equation (26) can be adopted to calculate h for the segment between the interface tip and the no-flow boundary where $h = \phi$.

Similarly, the interface tip location of Unit 2 is obtained by substituting equation (21a) into equation (14). Then, the value of h for the aquifer segment between the interface tip and no-flow boundary for Unit 2 is computed by repeating the steps from equations (22) to (26).

4. Results and Discussion

4.1. Validation of Analytical Solutions

The analytical solutions were validated by comparing their predictions with experimental data compiled from Memari et al. (2020). Their experiments were carried out using a 15° radial tank that can be considered as an ASA. The radial tank contained three distinct chambers: no-flow boundary condition, porous medium and seaward boundary condition. The no-flow and seaward boundaries were respectively located at 10 cm and 55.5 cm from the circle center, i.e., 45.5 cm from the no-flow boundary to seaward boundary along the radial direction (L^*). Note that the experimental tank only corresponds to Unit 1 of the radial aquifer with $l_1 = L^*$ while $l_2 = 0$ cm. The thickness of the porous medium and sea level were 28 and 25 cm, respectively. The sand used in experiments had a saturated hydraulic conductivity of 1.23 × 10^{-2} m/s and an effective porosity of 0.40. The measured saltwater and freshwater densities were respectively 1.015 and 0.999 g/ml, leading to $\alpha = 62$. Two different recharge events, 2.46 × 10^{-4} m/s and 1.08 × 10^{-4} m/s, were considered in the experiments. For clarity, experimental parameters are summarized in Table 1.

Figure 3 shows the comparison between analytical and experimental results of the freshwater-seawater interface for different recharge events. In general, the analytical solution performs well in predicting the freshwater-seawater interface for both recharge events, despite that there are small differences between analytical results and measurements, particularly in the zone near the sea boundary. These deviations are likely due to assumptions made in the analytical solution, i.e., (i) a sharp freshwater-seawater interface, (ii) ignoring the effect of freshwater discharge, and (iii) neglecting the vertical flow.

4.2. Effects of Aquifer Geometry on Seawater Intrusion

Previous studies indicated that boundary conditions play a critical role in affecting seawater intrusion (Werner & Simmons, 2009; Lu et al., 2016). Therefore, the no-flow

https://doi.org/10.5194/hess-2021-29
Preprint. Discussion started: 11 March 2021

boundary between the sea and lagoon was examined for ASAs. As indicated by equations (16) and (17), this no-flow boundary only depends on L and L_0. The values of l_1 and l_2 calculated respectively from equations (16) and (17) are shown in Figure 4 for three typical values of L (500, 1000 and 2000 m) with varying L_0 from 10^2 to 10^6 m. In general, the no-flow boundary deviates from the middle of the ASA. When L_0 is smaller than 10^5 m, l_1 is larger than l_2 for the three different values of L, indicating a no-flow boundary closer to the lagoon boundary. For example, assuming L = 2000 m and L_0 = 100 m leads to l_1 = 1240 m and l_2 = 760 m, with a deviation of 240 m (12% of 2000 m) from the middle of the ASA. When L_0 exceeds 10^5 m, however, the no-flow boundary can be approximated to be at the middle of the ASA for all considered values of L. This is in contrast to strip and circular aquifers where the no-flow boundary is in the middle of aquifers due to symmetric flow. Moreover, l_1 approaches l_2 with increasing L_0, which suggests a movement of the no-flow boundary to the middle of the ASA. This is because, as L_0 increases, the island shape approaches to be rectangular and hence leading to the flow parallel with EH and FG. By comparison, at a given L_0 smaller than 10^5 m, the no-flow boundary location deviates more from the middle of the ASA with increasing L.

Since the no-flow boundary location between the sea and lagoon deviates from the middle of the ASA, we expect aquifer geometry to play a significant role in controlling seawater intrusion. As mentioned previously, ASAs can be convergent (Unit 1) or divergent aquifers (Unit 2) where the extent of seawater intrusion may be different. However, for strip aquifers, both Units 1 and 2 are rectangular with the same extent of seawater intrusion. Therefore, three geometries were compared in this study: convergent, rectangular and divergent (Figure 5).

https://doi.org/10.5194/hess-2021-29
Preprint. Discussion started: 11 March 2021

Hydrology and Earth System Sciences
Open Access
EGU
Discussions

These geometries have been widely examined in hillslope hydrology regrading to the effects of aquifer geometry on runoff generation (Troch et al., 2003; Kong et al., 2016; Luo et al., 2018). For the sake of simplicity, we replaced the *x*-*z* coordinate origin at the intersection of the seawater boundary and the impermeable base, with the *x*-axis horizontally pointing to the no-flow boundary and the *z*-axis vertically upward.

Following previous studies (e.g., Lu et al., 2016; 2019), hypothesized cases were designed to show the effects of aquifer geometry on seawater intrusion (Cases 1 and 2 in Table 1). According to Werner et al. (2017), the width of atoll islands generally varies from 100 to 1500 m along the radial direction. In order to focus on the effects of aquifer geometry on seawater intrusion, we assumed the same L^* and L_0 for the three aquifers, with L^* and L_0 equal to 1000 and 200 m, respectively. The sand characteristics were the same as in the experiments of Memari et al. (2020). Two recharge events were considered (Cases 1 and 2, Table 1). The freshwater-seawater interface was calculated using the analytical solutions for the three different aquifers. Note that Appendix A presents analytical solutions for seawater intrusion in strip aquifers deduced from Lu et al. (2019).

Figure 6 shows the freshwater-seawater interface calculated for Cases 1 and 2. As can be seen, the extent of seawater intrusion is greatly different for the three different aquifers. For the high recharge, the interface tip is located at around 500 m for the divergent aquifer, about twice the value of the rectangular aquifer and six times the value for the convergent aquifer (Figure 6a). When the recharge decreases to 3×10^{-7} m/s, the interface tip moves more landward for three aquifers as expected, but the difference between results of three aquifers is still great

(Figure 6b). The interface tip rises above the aquifer bed for both rectangular and divergent aquifers, while it remains on the aquifer bed for the convergent aquifer. Regardless of the recharge rate, the most landward freshwater-seawater interface occurs in divergent aquifers and vice versa for convergent aquifers. This underlines that aquifer geometry plays a significant role in controlling seawater intrusion and hence it is necessary to account for the effects of aquifer geometry in analytical solutions of seawater intrusion.

4.3. Sensitivity Analysis

A sensitivity analysis was conducted to investigate at which degree of curvature the deviation of seawater intrusion between three different aquifers becomes significant. Since we focus on the effects of aquifer geometry on seawater intrusion, values of L_0 and L^* were varied, with other parameters kept constant. When conducting the sensitivity analysis of L_0, L^* was fixed at 1000 m that is a typical value for ASAs (Werner et al., 2017). Figure 7 shows the sensitivity of the freshwater-seawater interface and watertable elevation to changes in L_0 (Case 3, Table 1). As expected, the freshwater-seawater interface and watertable elevation are independent of L_0 for rectangular aquifers. However, the freshwater-seawater interface and watertable elevation differ greatly when varying L_0 for both convergent and divergent aquifers, highlighting that L_0 plays an important role in affecting seawater intrusion. Specifically, as L_0 increases, the freshwater-seawater interface moves more landward (Figure 7a) and its corresponding watertable elevation decreases (Figure 7c) for convergent aquifers. This is contrary to divergent aquifers where the freshwater-seawater interface moves more seaward (Figure 7b) and its corresponding watertable elevation increases (Figure 7d) with increasing L_0.

For a given L_0, divergent aquifers have the largest extent of seawater intrusion and lowest watertable elevation, and conversely for convergent aquifers (Figure 7). Consistent with the experimental results of Hilberts et al. (2005), the steady-state watertable elevation is lower in the divergent aquifer than in the convergent aquifer for the same rainfall.

By comparison, the deviation between rectangular aquifers and divergent or convergent aquifers, regardless of the freshwater-seawater interface and watertable elevation, is significant when L_0 is less than 2000 m (Figure 7). For example, the interface toe location is 262 m for the rectangular aquifer at L_0 = 200 m, whereas it is 78 m (31% of that in the rectangular aquifer) and 500 m (191% of that in the rectangular aquifer) for the convergent and divergent aquifers, respectively. As L_0 increase, the deviation between three aquifers decreases. When L_0 = 2000 m, the interface toe location is 262, 209 (80% of that in the rectangular aquifer) and 318 m (121% of that in the rectangular aquifer), respectively. As L_0 continues to increase to 6000 m, the freshwater-seawater interface and watertable elevation of both convergent and divergent aquifers tend to those of rectangular aquifers, i.e., geometry effects decrease with increasing L_0. These highlight the critical role played by the shape of aquifers. As a result, ignoring geometry effects may lead to an inappropriate management strategy for fresh groundwater resource in atoll islands.

The sensitivity of the freshwater-seawater interface and watertable elevation to L^* was further conducted with varying L^* from 600 to 1600 m while fixing L_0 at 200 m (Case 4, Table 1). As shown in Figure 8, in contrary to L_0, the freshwater-seawater interface and watertable elevation in all three topographies is related to L^*. Again, seawater intrusion is greatest in divergent aquifers and least in convergent aquifers for given L^*. When L^* increases, the freshwater-seawater interface moves more seaward and the watertable elevation increases, regardless of aquifer geometry, i.e., the seawater intrusion decreases (Figure 8a-c). This is because the total freshwater flux increases with increasing L^*, leading to a higher hydraulic gradient and hence less seawater intrusion (Figures 8d-f). Moreover, an increase in L^* induces a smaller deviation of seawater intrusion between three geometries, i.e., geometry effects on seawater intrusion are more significant at small L^*. However, even at the maximum L^* given in this study (1600 m), the deviation between three aquifers is significant: the interface toe location is about 148 m for the rectangular aquifer, whereas it is about 32 (22% of that in the rectangular aquifer) and 278 m (188% of that in the rectangular aquifer) for the convergent and divergent aquifers, respectively. Both L_0 and L^* can greatly impact seawater intrusion for divergent and convergent aquifers, highlighting the necessity to include geometry effects into analytical solutions of seawater intrusion.

4.4. Limitations of This Study and Future Work

The foregoing results show that aquifer geometry affects the freshwater-seawater interface and watertable elevation, and is directly related to the aquifer width, the distance from the circle center to the no-flow boundary, and aquifer shape, i.e., whether the aquifer is convergent or divergent. Of the aquifer shapes considered, divergent aquifers are the most vulnerable to seawater intrusion and convergent aquifers have the least seawater intrusion. Correspondingly, the watertable elevation is the lowest in divergent aquifers and highest in convergent aquifers, which is consistent with rainfall-runoff generation in unconfined hillslope aquifers (Hilberts et

https://doi.org/10.5194/hess-2021-29
Preprint. Discussion started: 11 March 2021

Hydrology and Earth System Sciences
Discussions

al., 2005; Hazenberg et al., 2015; Kong et al., 2016). The assumption of a rectangular aquifer may lead to inaccurate estimates of freshwater storage on oceanic islands and hence future efforts should be devoted to establishing digital elevation models with high accuracy for oceanic islands. Therefore, it is necessary to build the hydrology database for oceanic islands including soil properties, rainfall, sea level, water level of lagoon and others for estimating seawater intrusion accurately. Although some existing codes such as SEAWAT (Langevin et al., 2008) and SUTRA (Voss & Provost, 2008) can be used to simulate seawater intrusion in ASAs, they are computationally expensive, especially for divergent and convergent aquifers where the model domain cannot reduce to a two-dimensional section. However, the new analytical solutions, validated against experiments, can be used as a fast tool to estimate seawater intrusion in ASAs. Due to lack of data, the new analytical solutions have not been applied to estimate seawater intrusion in the field. Despite of this, it can be expected that the analytical solutions can be easily used once we have known island geometry and corresponding soil properties.

In line with previous studies, a variety of assumptions were made to facilitate deriving analytical solutions the freshwater-seawater interface and watertable elevation (e.g., Fetter, 1972; Strack, 1976; Lu et al., 2019). In addition to the assumptions mentioned previously, the temporal and spatial variability in recharge is not considered into analytical solutions. Previous field monitoring and numerical modelling studies in St. Georgia Island indicate that the freshwater lens morphology is controlled by spatial variability of recharge values, while the response of the freshwater lens to monthly variability in recharge is insignificant (Schneider & Kruse, 2006). In addition, the lagoon water level usually lags behind the sea level, leading to changes of the no-flow boundary condition that greatly affects seawater intrusion. Furthermore, global mean sea level has increased with an apparent rate acceleration during the last decade (Dieng et al., 2017; Kim et al., 2019), which further results in uncertainties to predict seawater intrusion in oceanic islands. The effects of temporal and spatial variability in recharge, water level difference between sea and lagoon and sea level rise on seawater intrusion in ASAs should be further explored in the future work.

5. Conclusions

Based on the Ghijben-Herzberg and hillslope-storage Boussinesq equations, we derived analytical solutions of steady-state seawater intrusion for ASAs, with a focus on the freshwater-seawater interface and its corresponding watertable elevation. After comparing with experimental data of Memari et al. (2020), the analytical solutions were employed to examine the effects of aquifer geometry on seawater intrusion in island aquifers. Three different shapes of island aquifer were compared: convergent, rectangular and divergent. The results lead to the following conclusions:

(1) The presented analytical solutions perform well in predicting the experimental freshwater-seawater interface for both recharge events, suggesting that these analytical solutions can predict seawater intrusion reasonably in different aquifer geometries.

(2) Island geometry plays a significant role in affecting the freshwater-seawater interface and watertable elevation. The extent of seawater intrusion is the most serious in divergent aquifers, while the lightest in convergent aquifers. In contrast, the watertable elevation is the lowest in divergent aquifers while the highest in convergent aquifers.

https://doi.org/10.5194/hess-2021-29
Preprint. Discussion started: 11 March 2021

Hydrology and Earth System Sciences
Open Access
Discussions

(3) The effects of aquifer geometry on seawater intrusion are dependent of the aquifer width and distance from the circle center to the no-flow boundary. Both a larger of the aquifer width and distance from the circle center to the no-flow boundary can weaken the role played by aquifer geometry and hence lead to a smaller deviation of the extent of seawater intrusion between three topographies.

Real island aquifers are expected to exhibit more complexity than considered here with regards to their topographies and subjecting to transient flow conditions caused by tide and wave. Nevertheless, based on steady-state analytical solutions, the present results provide the overall behavior of the effects of aquifer geometry on seawater intrusion. As the results show, the freshwater-seawater interface and watertable elevation within island aquifers can be markedly affected by aquifer geometry.

https://doi.org/10.5194/hess-2021-29
Preprint. Discussion started: 11 March 2021

Appendix A: Analytical Solutions for Rectangular Aquifers

For rectangular aquifers, seawater intrusion in Units 1 is identical to that in Unit 2 because of symmetrical groundwater flow. With the interface tip on the aquifer bed, analytical solutions of the freshwater-seawater interface, watertable elevation, and interface tip in Unit 2 can be respectively written as (Lu et al., 2019),

$$h_s = \alpha\sqrt{\frac{N}{(1+\alpha)K_s}\left(\frac{L^2}{4}-x^2\right)} \tag{A1}$$

$$h = \sqrt{\frac{N}{(1+\alpha)K_s}\left(\frac{L^2}{4}-x^2\right)}+H_s \quad \left(x_t < x \le \frac{L}{2}\right) \tag{A2}$$

$$h = \sqrt{\frac{N}{K_s}\left(x_t^2-x^2\right)+\left(\frac{H_s}{\alpha}+H_s\right)} \quad \left(0 \le x \le x_t\right) \tag{A3}$$

$$x_t = \sqrt{\frac{L^2}{4}-\frac{(1+\alpha)K_s}{N}\left(\frac{H_s^2}{\alpha^2}\right)} \tag{A4}$$

When the interface tip is above the aquifer bed, the analytical solution of the freshwater-seawater interface location and watertable elevation in Unit 2 are the same as equations (A1) and (A2), respectively.

https://doi.org/10.5194/hess-2021-29
Preprint. Discussion started: 11 March 2021

Hydrology and Earth System Sciences
Open Access
Discussions

Code/Data availability

The paper is theoretical, and experimental data used in this study can be found in Memari et al. (2020).

https://doi.org/10.5194/hess-2021-29
Preprint. Discussion started: 11 March 2021

Author contribution

All authors contributed to the design of the research. ZL carried out data collation, developed the analytical solutions and prepared the manuscript with contributions from all co-authors. All authors contributed to the interpretation of the results and provided feedback.

https://doi.org/10.5194/hess-2021-29
Preprint. Discussion started: 11 March 2021

Competing interests

The authors declare that they have no conflict of interest.

https://doi.org/10.5194/hess-2021-29
Preprint. Discussion started: 11 March 2021

Acknowledgments

This research was supported by the National Key R&D Program of China (2019YFC0409004), the Fundamental Research Funds for the Central Universities (2019B80714) and the National Natural Science Foundation of China (51979095). Z. L. acknowledges the China Scholarship Council for financial support (201906710039). J. K. acknowledges the Qing Lan Project of Jiangsu Province (2020).

https://doi.org/10.5194/hess-2021-29
Preprint. Discussion started: 11 March 2021

References

Ayers, J. F., & Vacher, H. L. (1986). Hydrogeology of an atoll island: A conceptual model from detailed study of a Micronesian example. *Groundwater*, *24*(2), 185-198. https://doi.org/10.1111/j.1745-6584.1986.tb00994.x

Badaruddin, S., Werner, A. D., & Morgan, L. K. (2015). Water table salinization due to seawater intrusion. *Water Resources Research,* *51*(10), 8397-8408. https://doi.org/10.1002/2015WR017098

Bailey, R. T., Jenson, J. W., & Olsen, A. E. (2010). Estimating the ground water resources of atoll islands. *Water*, *2*(1), 1-27. https://doi.org/10.3390/w2010001

Bailey, R. T., Jenson, J. W., & Olsen, A. E. (2009). Numerical modeling of atoll island hydrogeology. *Groundwater*, *47*(2), 184-196. https://doi.org/10.1111/j.1745-6584.2008.00520.x

Bedekar, V. S., Memari, S. S., & Clement, T. P. (2019). Investigation of transient freshwater storage in island aquifers. *Journal of Contaminant Hydrology*, *221*, 98-107. https://doi.org/10.1016/j.jconhyd.2019.02.004

Chesnaux, R., & Allen, D. M. (2008). Groundwater travel times for unconfined island aquifers bounded by freshwater or seawater. *Hydrogeology Journal*, *16*(3), 437-445. https://doi.org/10.1007/s10040-007-0241-6

Dieng, H. B., Cazenave, A., Meyssignac, B., & Ablain, M. (2017). New estimate of the current rate of sea level rise from a sea level budget approach. *Geophysical Research Letters*, *44*(8), 3744-3751. https://doi.org/10.1002/2017GL073308

Dose, E. J., Stoeckl, L., Houben, G. J., Vacher, H. L., Vassolo, S., Dietrich, J., & Himmelsbach, T. (2014). Experiments and modeling of freshwater lenses in layered aquifers: Steady state interface geometry. *Journal of Hydrology*, *509*, 621-630. https://doi.org/10.1016/j.jhydrol.2013.10.010

Drabbe J. & Badon Ghijben, W. (1889). *Nota in verband met de voorgenomen put boring nabij Amsterdam*, Tijdschr. Kon. Inst. Ing., pp. 8-22, Gravenhage, Netherlands.

Duvat, V. K. E. (2019). A global assessment of atoll island planform changes over the past decades. *Wiley Interdisciplinary Reviews: Climate Change*, *10*(1), e557. https://doi.org/10.1002/wcc.557

Fetter, C. W. (1972). Position of the saline water interface beneath oceanic islands. *Water Resources Research*, *8*(5), 1307-1315. https://doi.org/10.1029/WR008i005p01307

Gingerich, S. B., Voss, C. I., & Johnson, A. G. (2017). Seawater-flooding events and impact on freshwater lenses of low-lying islands: Controlling factors, basic management and mitigation. *Journal of Hydrology*, *551*, 676-688. https://doi.org/10.1016/j.jhydrol.2017.03.001

Greskowiak, J., Röper, T., & Post, V. E. (2013). Closed-form approximations for two-dimensional groundwater age patterns in a fresh water lens. *Groundwater*, *51*(4), 629-634. https://doi.org/10.1111/j.1745-6584.2012.00996.x

Hazenberg, P., Fang, Y., Broxton, P., Gochis, D., Niu, G. -Y., Pelletier, J. D., Troch, P. A., & Zeng, X. (2015). A hybrid-3D hillslope hydrological model for use in Earth system models. *Water Resources Research*, *51*(10), 8218-8239.

https://doi.org/10.5194/hess-2021-29
Preprint. Discussion started: 11 March 2021

https://doi.org/10.1002/2014WR016842

Herzberg, A. (1901). Die wasserversorgung einiger Nordseebäder (The water supply of some North Sea spas, in German). *Journal für Gasbeleuchtung und Wasserversorgung*, *44*, 815–819, *45*, 842-844.

Hilberts, A. G. J., Troch, P. A., & Paniconi, C. (2005). Storage-dependent drainable porosity for complex hillslopes. *Water Resources Research*, *41*(6). https://doi.org/10.1029/2004WR003725

Ketabchi, H., Mahmoodzadeh, D., Ataie-Ashtiani, B., Werner, A. D., & Simmons, C. T. (2014). Sea-level rise impact on fresh groundwater lenses in two-layer small islands. *Hydrological Processes*, *28*(24), 5938-5953. https://doi.org/10.1002/hyp.10059

Kim, J., Seo, K., Jeon, T., Chen, J., & Wilson, C. R. (2019). Missing hydrological contribution to sea level rise. *Geophysical Research Letters*, *46*(21), 12049-12055. https://doi.org/10.1029/2019GL085470

Kong, J., Shen, C., Luo, Z., Hua, G., & Zhao, H. (2016). Improvement of the hillslope-storage Boussinesq model by considering lateral flow in the unsaturated zone. *Water Resources Research*, *52*(4), 2965-2984. https://doi.org/10.1002/2015WR018054

Lam, R. K. (1974). Atoll permeability calculated from tidal diffusion. *Journal of Geophysical Research*, *79*(21), 3073-3081. https://doi.org/10.1029/JC079i021p03073

Langevin, C. D., Thorne Jr, D. T., Dausman, A. M., Sukop, M. C., & Guo, W. (2008). *SEAWAT version 4: A computer program for simulation of multi-species solute and heat transport* (No. 6-A22). U.S. Geological Survey. https://pubs.usgs.gov/tm/tm6a22/

https://doi.org/10.5194/hess-2021-29
Preprint. Discussion started: 11 March 2021

Hydrology and Earth System Sciences
Discussions

Liu, J., & Tokunaga, T. (2019). Future risks of tsunami-induced seawater intrusion into unconfined coastal aquifers: Insights from numerical simulations at Niijima Island, Japan. *Water Resources Research*, *55*(12), 10082-10104. https://doi.org/10.1029/2019WR025386

Lu, C., Cao, H., Ma, J., Shi, W., Rathore, S. S., Wu, J., & Luo, J. (2019). A proof-of-concept study of using a less permeable slice along the shoreline to increase fresh groundwater storage of oceanic islands: Analytical and experimental validation. *Water Resources Research*, *55*(8), 6450-6463. https://doi.org/10.1029/2018WR024529

Lu, C., Xin, P., Kong, J., Li, L., & Luo, J. (2016). Analytical solutions of seawater intrusion in sloping confined and unconfined coastal aquifers. *Water Resources Research*, *52*(9), 6989-7004. https://doi.org/10.1002/2016WR019101

Luo, Z., Shen, C., Kong, J., Hua, G., Gao, X., Zhao, Z., Zhao, H., & Li, L. (2018). Effects of unsaturated flow on hillslope recession characteristics. *Water Resources Research*, *54*(3), 2037-2056. https://doi.org/10.1002/2017WR022257

Memari, S. S., Bedekar, V. S., & Clement, T. P. (2020). Laboratory and numerical investigation of saltwater intrusion processes in a circular island aquifer. *Water Resources Research*, *56*(2). https://doi.org/10.1029/2019WR025325

Morgan, L. K., & Werner, A. D. (2014). Seawater intrusion vulnerability indicators for freshwater lenses in strip islands. *Journal of Hydrology*, *508*, 322-327. https://doi.org/10.1016/j.jhydrol.2013.11.002

Paniconi, C., Troch, P. A., Van Loon, E. E., & Hilberts, A. G. (2003). Hillslope-storage

Boussinesq model for subsurface flow and variable source areas along complex hillslopes: 2. Intercomparison with a three-dimensional Richards equation model. *Water Resources Research*, *39*(11). https://doi.org/10.1029/2002WR001730

Post, V. E. (2018). Annotated translation of “Nota in verband met de voorgenomen putboring nabij Amsterdam [Note concerning the intended well drilling near Amsterdam]” by J. Drabbe and W. Badon Ghijben (1889). *Hydrogeology Journal*, *26*(6), 1771-1788. https://doi.org/10.1007/s10040-018-1797-z

Post, V. E. A., Houben, G. J., Stoeckl, L., & Sültenfuß, J. (2019). Behaviour of tritium and tritiogenic helium in freshwater lens groundwater systems: Insights from Langeoog Island, Germany. *Geofluids*, *2019*, 1-16. https://doi.org/10.1155/2019/1494326

Röper, T., Greskowiak, J., Freund, H., & Massmann, G. (2013). Freshwater lens formation below juvenile dunes on a barrier island (Spiekeroog, Northwest Germany). *Estuarine, Coastal and Shelf Science*, *121-122*, 40-50. https://doi.org/10.1016/j.ecss.2013.02.004

Schneider, J. C., & Kruse, S. E. (2006). Assessing selected natural and anthropogenic impacts on freshwater lens morphology on small barrier islands: Dog Island and St. George Island, Florida, USA. *Hydrogeology Journal*, *14*(1-2), 131-145. https://doi.org/10.1007/s10040-005-0442-9

Stagnitti, F., Parlange, M. B., Steenhuis, T. S., & Parlange, J.-Y. (1986). Drainage from a uniform soil layer on a hillslope. *Water Resources Research*, *22*(5), 631-634. https://doi.org/10.1029/WR022i005p00631

Stoeckl, L., Houben, G. J., & Dose, E. J. (2015). Experiments and modeling of flow processes in freshwater lenses in layered island aquifers: Analysis of age stratification, travel times and interface propagation. *Journal of Hydrology*, *529*, 159-168. https://doi.org/10.1016/j.jhydrol.2015.07.019

Storlazzi, C. D., Gingerich, S. B., van Dongeren, A., Cheriton, O. M., Swarzenski, P. W., Quataert, E., Voss, C. I., Field, D. W., Annamalai, H., Piniak, G. A., & McCall, R. (2018). Most atolls will be uninhabitable by the mid-21st century because of sea-level rise exacerbating wave-driven flooding. *Science Advances*, *4*(4), eaap9741. https://doi.org/10.1126/sciadv.aap9741

Strack, O. D. L. (1976). A single-potential solution for regional interface problems in coastal aquifers. *Water Resources Research*, *12*(6), 1165-1174. https://doi.org/10.1029/WR012i006p01165

Stuyfzand, P. J. (2017). Observations and analytical modeling of freshwater and rainwater lenses in coastal dune systems. *Journal of Coastal Conservation*, *21*(5), 577-593. https://doi.org/10.1007/s11852-016-0456-6

Stuyfzand, P. J. (1993) *Hydrochemistry and hydrology of the coastal dune area of the Western Netherlands*. Ph.D. Thesis Vrije Univ. Amsterdam, published by KIWA, ISBN 90-74741-01-0. http://dare.ubvu.vu.nl/handle/1871/12716, 366 p

Thomas, A., Baptiste, A., Martyr-Koller, R., Pringle, P., & Rhiney, K. (2020). Climate change and small island developing states. *Annual Review of Environment and Resources*, *45*(1), 1–27. https://doi.org/10.1146/annurev-environ-012320-083355

Troch, P. A., Paniconi, C., & Emiel van Loon, E. (2003). Hillslope-storage Boussinesq model

https://doi.org/10.5194/hess-2021-29
Preprint. Discussion started: 11 March 2021

for subsurface flow and variable source areas along complex hillslopes: 1. Formulation and characteristic response. *Water Resources Research*, *39*(11). https://doi.org/10.1029/2002WR001728

Underwood, M. R., Peterson, F. L., & Voss, C. I. (1992). Groundwater lens dynamics of atoll islands. *Water Resources Research*, *28*(11), 2889-2902. https://doi.org/10.1029/92WR01723

Vacher, H. L. 1988. Dupuit-Ghyben-Herzberg analysis of strip-island lenses. *Bulletin Geological Society of America, 100*: 580-591.

Voss, C. I., & Provost, A. M. (2008). *SUTRA: A model for saturated-unsaturated, variable density groundwater flow with solute or energy transport* (Rep.02–4231). Reston, VA: U.S. Geological Survey. https://water.usgs.gov/nrp/gwsoftware/sutra/SUTRA_2_2-documentation.pdf

Werner, A. D., Sharp, H. K., Galvis, S. C., Post, V. E., & Sinclair, P. (2017). Hydrogeology and management of freshwater lenses on atoll islands: Review of current knowledge and research needs. *Journal of Hydrology*, *551*, 819-844. https://doi.org/10.1016/j.jhydrol.2017.02.047

Werner, A. D., Bakker, M., Post, V. E., Vandenbohede, A., Lu, C., Ataie-Ashtiani, B., Simmons, C. T., & Barry, D. A. (2013). Seawater intrusion processes, investigation and management: recent advances and future challenges. *Advances in Water Resources*, *51*, 3-26. https://doi.org/10.1016/j.advwatres.2012.03.004

Werner, A. D., & Simmons, C. T. (2009). Impact of sea-level rise on sea water intrusion in

https://doi.org/10.5194/hess-2021-29
Preprint. Discussion started: 11 March 2021

coastal aquifers. *Groundwater*, *47*(2), 197-204. https://doi.org/10.1111/j.1745-6584.2008.00535.x

White, I., & Falkland, T. (2010). Management of freshwater lenses on small Pacific islands. *Hydrogeology Journal*, *18*(1), 227-246. https://doi.org/10.1007/s10040-009-0525-0

Zhang, Y., Li, L., Erler, D. V., Santos, I., & Lockington, D. (2016). Effects of alongshore morphology on groundwater flow and solute transport in a nearshore aquifer. *Water Resources Research*, *52*(2), 990-1008. https://doi.org/10.1002/2015WR017420

https://doi.org/10.5194/hess-2021-29
Preprint. Discussion started: 11 March 2021

Hydrology and Earth System Sciences
Open Access
Discussions
EGU

614 

615 **Figure 1.** Island with an annulus segment in the Namu Atoll (© Google Earth).

https://doi.org/10.5194/hess-2021-29
Preprint. Discussion started: 11 March 2021

Hydrology and Earth System Sciences
Open Access
EGU
Discussions

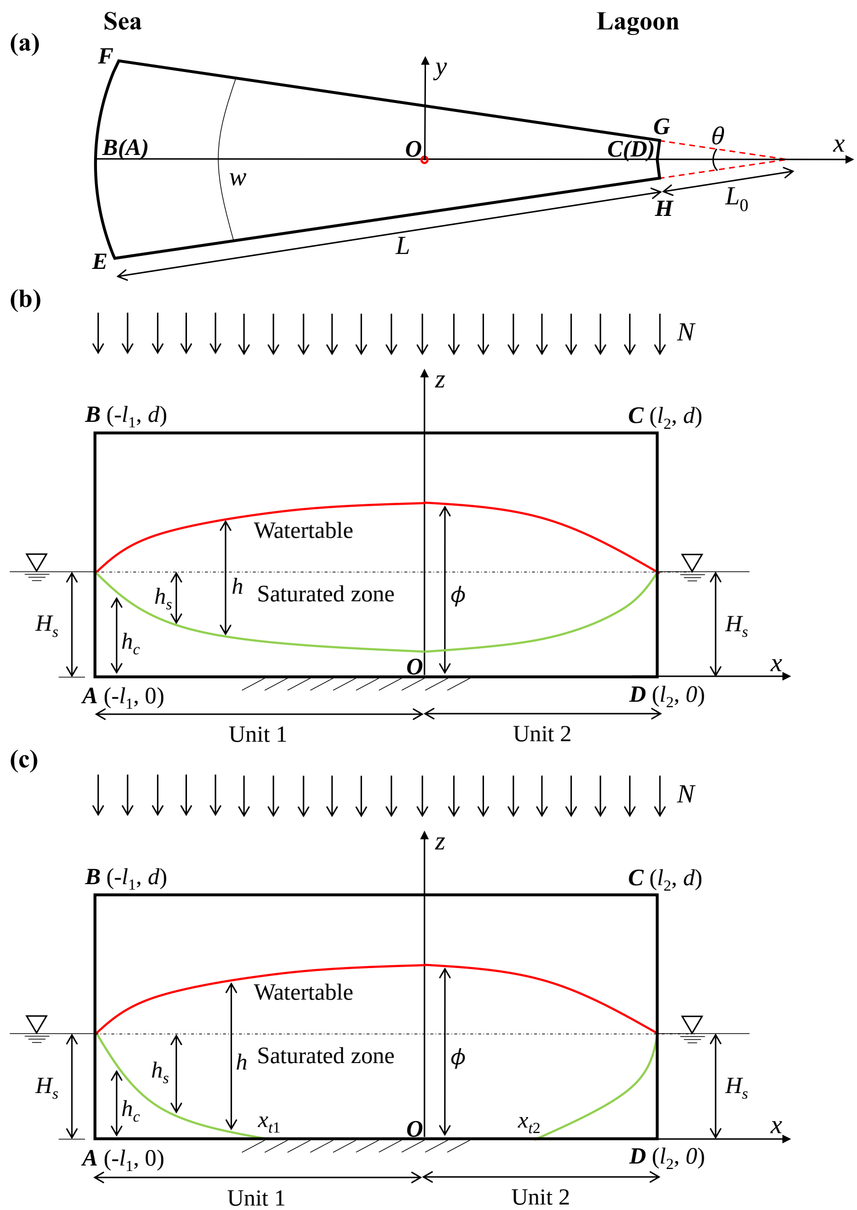

Figure 2. Conceptual model of an annulus segment aquifer (a slice of atoll islands). (a) Plain view and (b, c) side view with the saltwater interface tip (b) above the aquifer bed and (c) on the aquifer bed.

https://doi.org/10.5194/hess-2021-29
Preprint. Discussion started: 11 March 2021

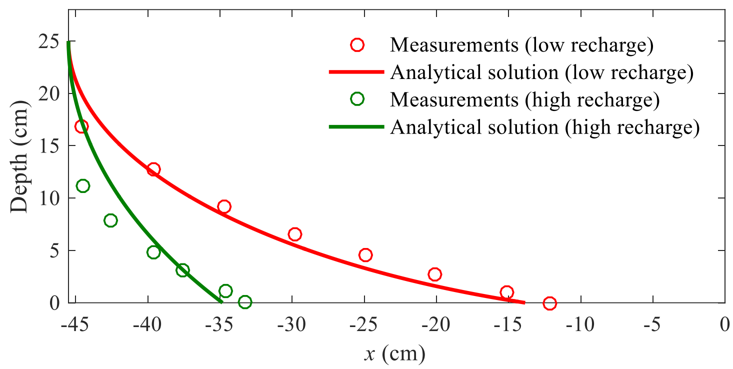

Figure 3. Comparison between analytical and experimental results of the freshwater-seawater interface for different recharge events. Note that the left and right sides are the sea and no-flow boundaries, respectively.

https://doi.org/10.5194/hess-2021-29
Preprint. Discussion started: 11 March 2021

Hydrology and Earth System Sciences
Open Access
EGU
Discussions

624 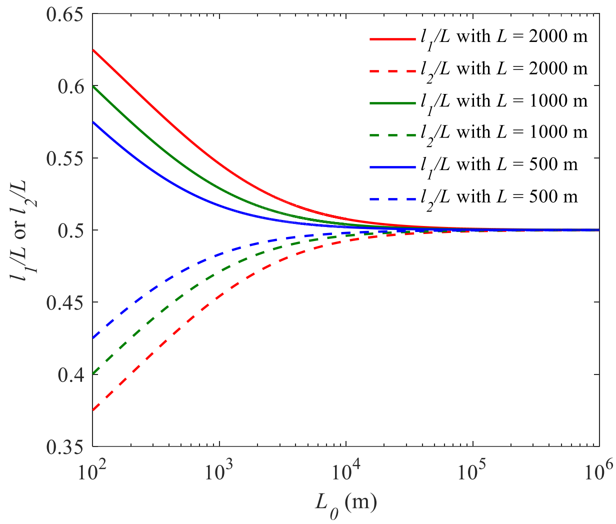

625 **Figure 4.** Widths of Unit 1 and Unit 2 versus L_0 for aquifers with different total width L.

https://doi.org/10.5194/hess-2021-29
Preprint. Discussion started: 11 March 2021

Hydrology and Earth System Sciences
Discussions

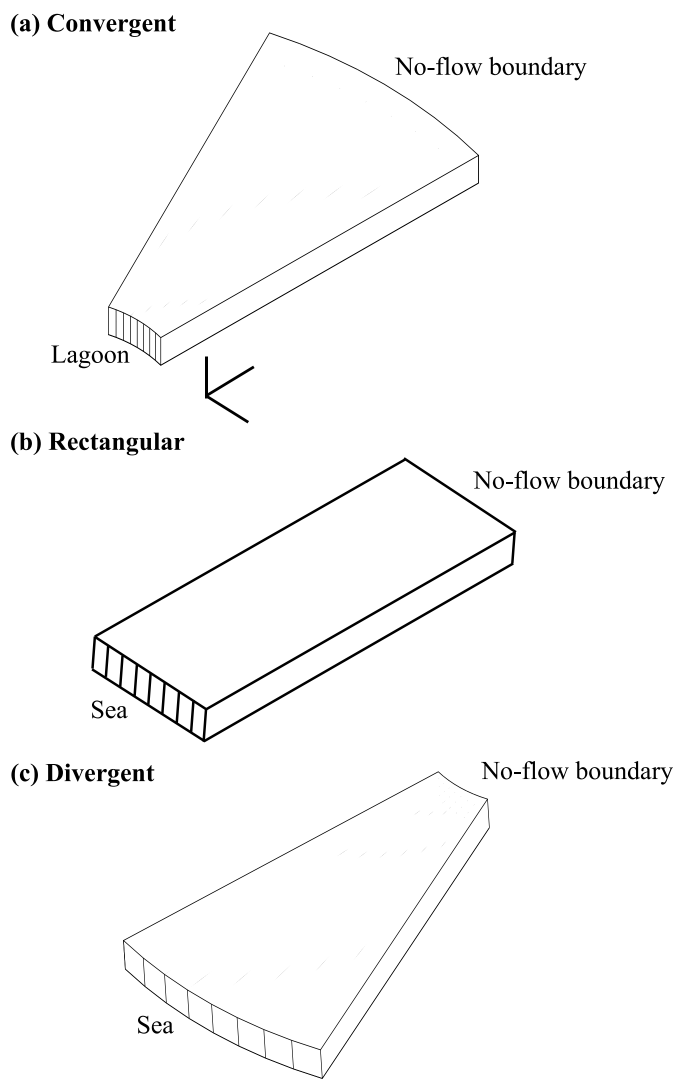

Figure 5. Three-dimensional view of (a) convergent (smaller side facing the lagoon), (b) rectangular and (c) divergent aquifers (larger side facing the sea) compared in this study. Note that the left and right sides of the aquifer are the sea and no-flow boundaries, respectively.

https://doi.org/10.5194/hess-2021-29
Preprint. Discussion started: 11 March 2021

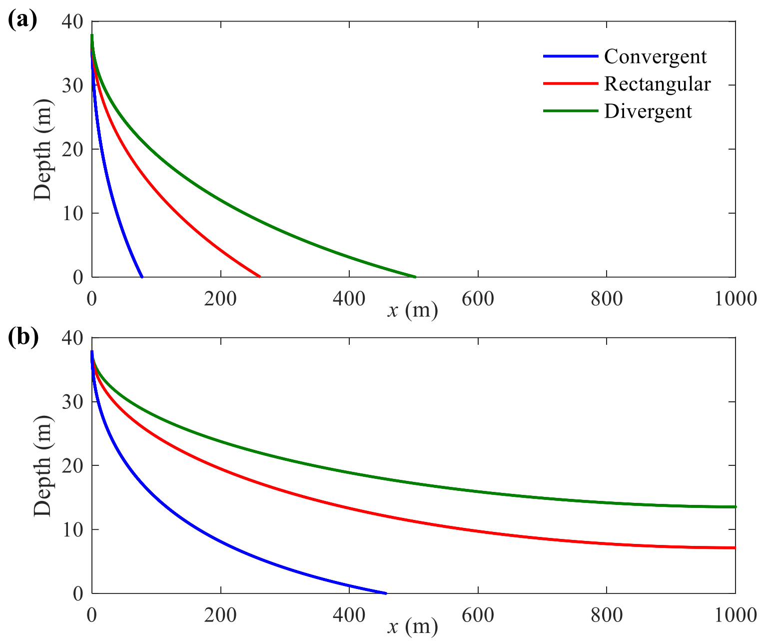

Figure 6. Freshwater-seawater interface predicted by analytical solutions for three different aquifers with (a) high and (b) low recharge.

https://doi.org/10.5194/hess-2021-29
Preprint. Discussion started: 11 March 2021

Hydrology and Earth System Sciences
Open Access
EGU
Discussions

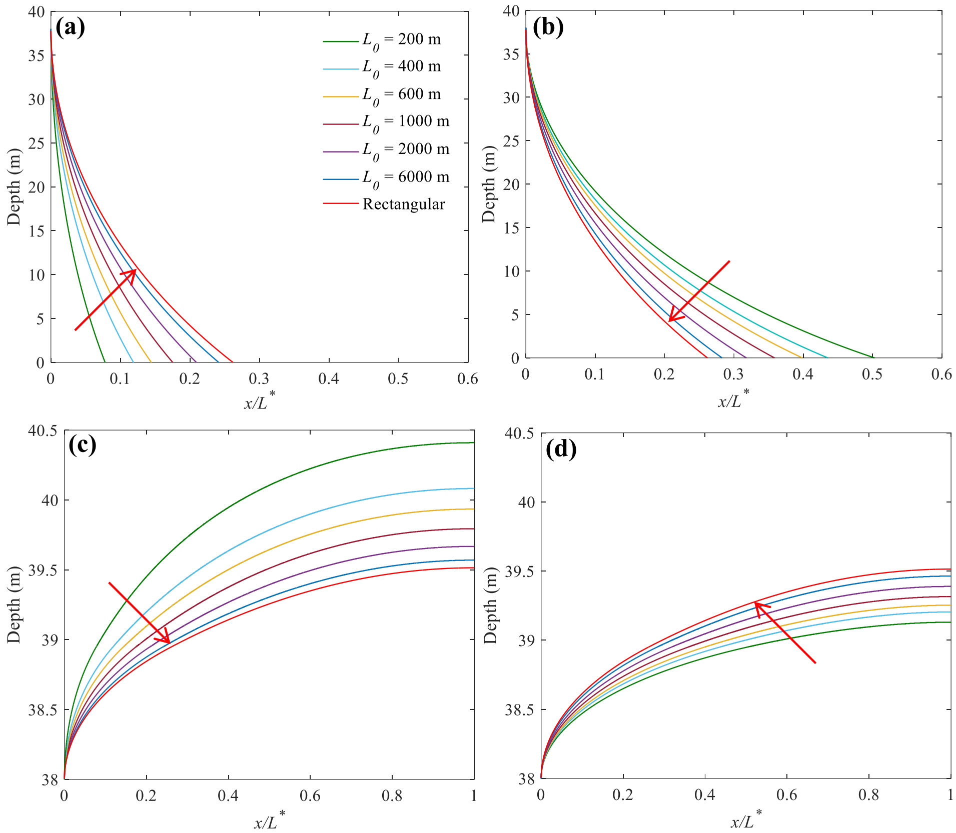

Figure 7. Sensitivity of (a, b) the freshwater-seawater interface and (c, d) watertable to L_0 for convergent (left panel) and divergent (right panel) aquifers. Note that red arrows point to the increase of L_0.

https://doi.org/10.5194/hess-2021-29
Preprint. Discussion started: 11 March 2021

Hydrology and Earth System Sciences Discussions

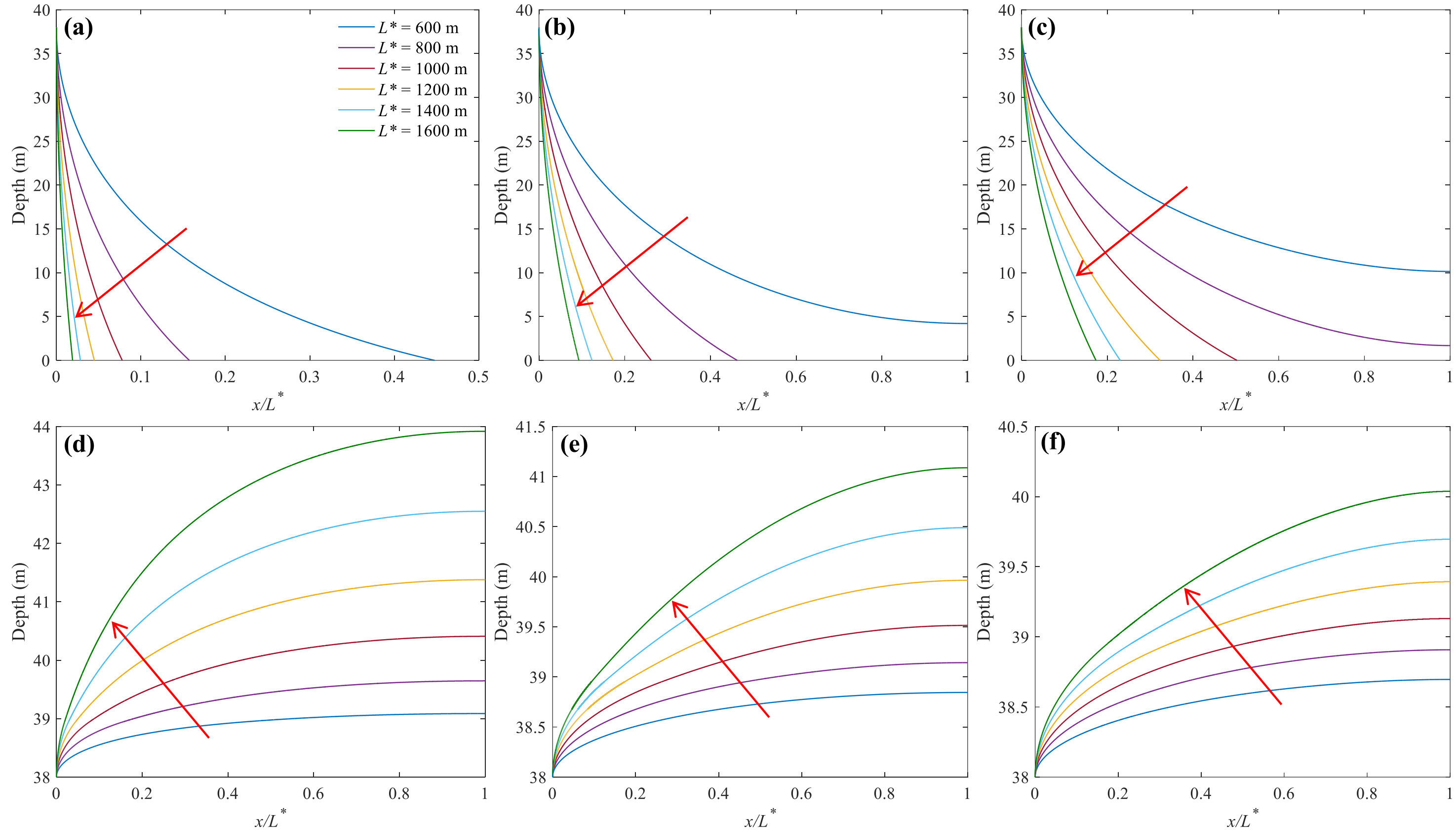

Figure 8. Sensitivity of (a-c) the freshwater-seawater interface and (d-f) watertable to L^* for convergent (left panel), rectangular (middle panel) and divergent (right panel) aquifers. Note that red arrows point to the increase of L^*.

https://doi.org/10.5194/hess-2021-29
Preprint. Discussion started: 11 March 2021

Hydrology and Earth System Sciences
Discussions
Open Access
EGU

Table 1. List of parameters.

	NO.	L^* (m)	L_0 (m)	H_s (m)	d (m)	α (-)	n_e (-)	K_s (m/s)	N (m/s)
Experiments	1	0.455	0.1	0.25	0.28	62	0.4	1.23×10^{-2}	2.46×10^{-4}
	2	0.455	0.1	0.25	0.28	62	0.4	1.23×10^{-2}	1.08×10^{-4}
Hypothesized Cases	1	1000	200	38	45	40	0.4	1.23×10^{-2}	1×10^{-6}
	2	1000	200	38	45	40	0.4	1.23×10^{-2}	3×10^{-7}
	3	1000	-	38	45	40	0.4	1.23×10^{-2}	1×10^{-6}
	4	-	200	38	45	40	0.4	1.23×10^{-2}	1×10^{-6}

Note: - means that the parameter is varied.